DNA–Tentacle Porphyrin Interactions: AT Over GC Selectivity Exhibited by an Outside Binding Self-Stacking Porphyrin

Nancy E. Mukundan,[†] Gabor Pethö,[†,‡] Dabney W. Dixon,*[,§] and Luigi G. Marzilli*[,†]

Departments of Chemistry, Emory University, Atlanta, Georgia 30322, and Georgia State University, Atlanta, Georgia 30303

Received September 14, 1994[⊗]

The binding characteristics of the tentacle porphyrin TθOPP (*meso*-tetrakis[4-[(3-(trimethylammonio)propyl)-oxy]phenyl]porphyrin) to [poly(dA-dT)]$_2$ and to [poly(dG-dC)]$_2$ were investigated. TθOPP differs from other porphyrins studied with DNA in having the positive charges on a flexible group, i.e. the tentacle. We assessed whether the DNA binding of such a species could be influenced by the sequence. In previous studies with calf thymus (CT) DNA, TθOPP was found to bind in a nonintercalative outside binding mode with self-stacking increasingly important at higher ratios of TθOPP to base pairs. Decreases in absorbance and strong induced conservative CD signals in the Soret region characteristic of outside self-stacking were found here with [poly-(dA-dT)]$_2$ and [poly(dG-dC)]$_2$; thus, the mode of binding was outside self-stacking to both polymers. The resulting spectra for the two polymers were found to be sufficiently different to allow competitive binding studies, which showed preferential binding of TθOPP to [poly(dA-dT)]$_2$ over [poly(dG-dC)]$_2$. The visible and induced CD spectra of TθOPP bound to [poly(dA-dT)]$_2$ were similar to those reported for TθOPP bound to CT DNA, indicating that binding to CT DNA may be at AT sites. With [poly(dG-dC)]$_2$, self-stacking was more extensive than with [poly(dA-dT)]$_2$ or with CT DNA, as indicated by broad Soret bands and low-intensity CD signals. Furthermore, in high salt (100 mM NaCl), some of the spectral differences between the TθOPP–[poly(dG-dC)]$_2$ adduct and the other DNA adducts were even more pronounced. Unlike in previous examples of AT binding selectivity by porphyrins, the UV CD spectra of the DNA polymers did not change significantly. As found previously for CT DNA, the bound, protonated form of TθOPP has a positive, nonconservative CD band with [poly(dA-dT)]$_2$, indicative of non-self-stacked outside binding. However, the induced CD band associated with the [poly(dG-dC)]$_2$-bound, protonated form of TθOPP was conservative, indicating an unusual, possibly self-stacked, outside bound species. Our results demonstrate that even for a tentacle porphyrin and its protonated form, sequence has a significant effect on binding affinity and binding mode. Unlike in previous studies with metalloporphyrins that are more rigid than TθOPP and distort DNA, this selectivity probably arises from differences in the surface and hydration state of relatively undistorted DNA. Thus, TθOPP is a better probe of DNA features.

Introduction

The interactions of water-soluble porphyrins with nucleic acids have been the subject of many recent investigations.[1–3] The porphyrin–DNA binding model proposed by Fiel and co-workers indicates three possible binding modes: intercalation, simple outside binding, and outside binding with self-stacking of the porphyrin.[4] Partial intercalation may be considered to be a fourth possible binding mode.[5] Investigations into the dependence of the binding on base pair composition, *e.g.* AT vs GC sites, have been informative about the nature of the porphyrin–DNA binding interactions.[6–12] For example, studies of the binding of *meso*-tetrakis(4-*N*-methylpyridiniumyl)porphyrin (TMpyP(4), Chart 1) and its metal complexes to poly-(dA-dT)·poly(dA-dT) ([poly(dA-dT)]$_2$) and poly(dG-dC)·poly-(dG-dC) ([poly(dG-dC)]$_2$) have shown that intercalation of these porphyrins could occur at GC base pair sites, while at AT sites binding was external.[6–8]

Chart 1

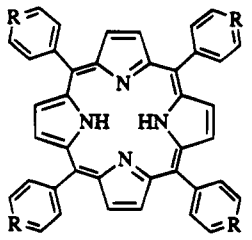

TMpyP(4) R = N^+-CH_3
TθOPP R = C-O$(CH_2)_3N^+(CH_3)_3$

The evaluation of possible binding sites and binding modes to homogeneous DNAs such as [poly(dA-dT)]$_2$ and [poly(dG-

* To whom correspondence should be addressed.
† Emory University.
‡ On leave from the Institute for Pharmaceutical Chemistry, Semmelweis Medical School, H-1092 Budapest, Hungary.
§ Georgia State University.
⊗ Abstract published in *Advance ACS Abstracts,* June 15, 1995.

(1) Fiel, R. J. *J. Biomol. Struct. Dyn.* **1989**, *6*, 1259–1274.
(2) Pasternack, R. F.; Gibbs, E. J. In *Metal-DNA Chemistry*; ACS Symposium Series 402; Tullius, T. D., Ed.; American Chemical Society: Washington, DC, 1989; pp 59–73.
(3) Marzilli, L. G. *New J. Chem.* **1990**, *14*, 409–420.
(4) Carvlin, M. J.; Fiel, R. J. *Nucleic Acids Res.* **1983**, *11*, 6121–6139.
(5) Ford, K. G.; Pearl, L. H.; Neidle, S. *Nucleic Acids Res.* **1987**, *15*, 6553–6562.
(6) Pasternack, R. F.; Gibbs, E. J.; Villafranca, J. J. *Biochemistry* **1983**, *22*, 2406–2414.
(7) Pasternack, R. F.; Gibbs, E. J.; Villafranca, J. J. *Biochemistry* **1983**, *22*, 5409–5417.
(8) Marzilli, L. G.; Banville, D. L.; Zon, G.; Wilson, W. D. *J. Am. Chem. Soc.* **1986**, *108*, 4188–4192.
(9) Strickland, J. A.; Marzilli, L. G.; Gay, K. M.; Wilson, W. D. *Biochemistry* **1988**, *27*, 8870–8878.
(10) Dougherty, G.; Pasternack, R. F. *Biophys. Chem.* **1992**, *44*, 11–19.
(11) Strahan, G. D.; Lu, D.; Tsuboi, M.; Nakamoto, K. *J. Phys. Chem.* **1992**, *96*, 6450–6457.
(12) Lin, M.; Lee, M.; Yue, K. T.; Marzilli, L. G. *Inorg. Chem.* **1993**, *32*, 3217–3226.

0020-1669/95/1334-3677$09.00/0

dC)]$_2$ is straightforward in comparison with heterogeneous DNAs like calf thymus (CT) DNA. Certain porphyrins have been found to bind more strongly to [poly(dA-dT)]$_2$ than to [poly(dG-dC)]$_2$.[9,12] The binding of ZnTMpyP(4) to [poly(dA-dT)]$_2$ was found to be ~200 times more favorable than to [poly(dG-dC)]$_2$.[9] From a separate linear dichroism study, it was proposed that ZnTMpyP(4) induced bends and kinks in the DNA at binding sites.[13] Therefore, a model was presented in which ZnTMpyP(4) binds to AT regions of DNA, possibly in the minor groove, producing changes in the conformation of the DNA;[9] these conformational changes are not as favored at GC sites. Similar AT selectivity was found with VOTMpyP(4) in competitive binding studies with [poly(dA-dT)]$_2$ and [poly(dG-dC)]$_2$.[12] Binding of ZnTMpyP(4) and VOTMpyP(4) to [poly(dA-dT)]$_2$ produced changes in the UV CD signals of the DNA itself, indicating that the DNA structure was distorted by the outside binding of these porphyrins. However, no such UV CD signal changes were observed in the spectrum of [poly(dG-dC)]$_2$ upon binding of VOTMpyP(4). Several outside binding cobalt porphyrins were proposed to bind at partially melted, most likely AT-rich regions of DNA.[14] The high-melting GC polymer has better stacking interactions and is less flexible than the low-melting AT polymer.

The porphyrins that have been shown to exhibit high AT selectivity[9,12] have axial ligands and do not effectively self-stack.[12] The positive charges are held rigidly at a fixed distance from the core; a reasonable hypothesis accounting for the AT selectivity is that the greater flexibility of the [poly(dA-dT)]$_2$ polymer permits better electrostatic interactions between the negatively charged phosphate groups and the rigidly fixed positive charges on the porphyrin. The UV CD spectrum of [poly(dA-dT)]$_2$ was significantly changed by these relatively rigid porphyrins.[9,12] We wanted to determine if such binding selectivity would be observed with a less rigid porphyrin.

We have reported on the binding characteristics of the porphyrin *meso*-tetrakis[4-[3-(trimethylammonio)propyl)oxy]-phenyl]porphyrin (TθOPP, Chart 1) to CT DNA.[15-17] The substituents of this tetracationic porphyrin are comprised of a trimethylammonium group attached to the end of a propyl chain, which is connected to the porphyrin core by a phenoxy group. Due to their relatively long, flexible nature, these substituents have been termed "tentacles". One might anticipate that the positive charges at the ends of the tentacles of TθOPP could form favorable electrostatic interactions with the mononegative DNA phosphodiester groups without necessarily distorting the DNA.

Our previous studies with TθOPP have ruled out intercalation.[15-17] We believe that the electron-richness of the core of TθOPP acts to stabilize the self-stacked, outside bound DNA adduct, disfavoring intercalation. A closely related porphyrin, TθpyP, which has the porphyrin core of TMpyP(4) and the tentacle arms of TθOPP, was found to intercalate into GC regions.[15] Thus, porphyrins with electron deficient cores such as TMpyP(4) or TθpyP appear to intercalate preferentially into GC regions. The compositional selectivity of outside binding for the tentacle porphyrin, TθOPP, has not been studied. The principal objective of this study is to elucidate binding selectivity for a purely outside binding tentacle porphyrin.

A few cationic porphyrins other than TθOPP have been found to bind to DNA in this self-stacked mode, including *meso*-tetrakis(4-trimethylaniliniumyl)porphyrin (TMAP),[4,18] *trans*-bis-(4-*N*-methylpyridiniumyl)diphenylporphyrin (*trans*-P(4)),[19,20] and the copper complex of TMpyP(4).[21] However, TMAP stacks under very limited circumstances, and *trans*-P(4) can intercalate under some conditions. Therefore, TθOPP affords a unique opportunity to study the effect of DNA composition on the binding of an outside bound self-stacked species.

In previous DNA binding studies of TθOPP with CT DNA (~42% of the base pairs are GC), we found that the bound TθOPP was protonated at relatively high pH since the bound form has a pK_a substantially higher than that of the free TθOPP.[16,17] Conditions favoring self-stacking of TθOPP were found to inhibit protonation. The spectral features of the bound protonated porphyrin were most consistent with a nonstacked binding mode. The relationships of the extent of protonation and of binding mode to polymer base pair composition are also of interest.

Experimental Section

Materials. TθOPP was prepared as previously described.[17] Solutions of TθOPP must be handled carefully since TθOPP readily adheres to glass. Both [poly(dA-dT)]$_2$ and [poly(dG-dC)]$_2$ were used as received from Pharmacia. Stock solutions of these polymers were prepared by dissolving the DNA in the appropriate volume of 10 mM NaCl. Their concentrations in base pairs were determined by UV spectroscopy ($\epsilon_{262} = 1.32 \times 10^4$ M^{-1} cm^{-1} for [poly(dA-dT)]$_2$[22] and $\epsilon_{254} = 1.68 \times 10^4$ M^{-1} cm^{-1} for [poly(dG-dC)]$_2$[23]). All DNA solutions were stored at −20 °C and were allowed to warm to room temperature before sample preparation.

PIPES (piperazine-*N*,*N*′-bis[2-ethanesulfonic acid]), MES (*N*-morpholineethanesulfonic acid) (both from SIGMA), and diphenylthiocarbazone (J. T. Baker) were reagent grade and were used without further purification. Metal-free distilled water, used for all solutions, was prepared by exhaustive extraction with a carbon tetrachloride solution of diphenylthiocarbazone.

Instrumentation. The UV−visible absorbance spectra were recorded on a Varian Cary3 UV−vis spectrophotometer. CD spectra were recorded on a JASCO 600 spectropolarimeter; to reduce noise, four spectra were acquired in succession and averaged. Ambient temperature was used for both spectroscopic methods. The pH of all samples was monitored with a 701A type pH meter (Orion Research) with a combination glass electrode (Ingold Electrodes Inc.).

Methods. To prepare the porphyrin−DNA adduct, the porphyrin was first diluted in the appropriate salt/buffer solution. The DNA aliquots were directly added to $R = 0.25$, 0.05, or 0.01, where R is the ratio [porphyrin]/[DNA base pair]. Often, the CD and visible spectra were monitored as a function of time. When the spectra were not being recorded, the solutions were stored in the dark at room temperature.

Results

Visible Absorbance Spectroscopy. TθOPP without DNA. The visible absorbance spectrum of the free base form of TθOPP (**P**) has been characterized previously[16,17] and consists of a Soret band at 418 nm ($\epsilon = 5.5 \times 10^5$ M^{-1} cm^{-1}) and four Q bands

(13) Geacintov, N. E.; Ibanez, V.; Rougee, M.; Bensasson, R. V. *Biochemistry* **1987**, *26*, 3087−3092.
(14) Sehlstedt, U.; Kim, S. K.; Carter, P.; Goodisman, J.; Vollano, J. F.; Nordén, B.; Dabrowiak, J. C. *Biochemistry* **1994**, *33*, 417−426.
(15) Marzilli, L. G.; Pethö, G.; Lin, M.; Kim, M. S.; Dixon, D. W. *J. Am. Chem. Soc.* **1992**, *114*, 7575−7577.
(16) Pethö, G.; Elliott, N. B.; Kim, M. S.; Lin, M.; Dixon, D. W.; Marzilli, L. G. *J. Chem. Soc., Chem. Commun.* **1993**, 1547−1548.
(17) Mukundan, N. E.; Pethö, G.; Dixon, D. W.; Kim, M. S.; Marzilli, L. G. *Inorg. Chem.* **1994**, *33*, 4676−4687.
(18) Carvlin, M. J.; Datta-Gupta, N.; Fiel, R. J. *Biochem. Biophys. Res. Commun.* **1982**, *108*, 66−73.
(19) Gibbs, E. J.; Tinoco, I., Jr.; Maestre, M. F.; Ellinas, P. A.; Pasternack, R. F. *Biochem. Biophys. Res. Commun.* **1988**, *157*, 350−358.
(20) Pasternack, R. F.; Bustamante, C.; Collings, P. J.; Giannetto, A.; Gibbs, E. J. *J. Am. Chem. Soc.* **1993**, *115*, 5393−5399.
(21) Hudson, B. P.; Sou, J.; Berger, D. J.; McMillin, D. R. *J. Am. Chem. Soc.* **1992**, *114*, 8997−9002.
(22) Schmechel, D. E. V.; Crothers, D. M. *Biopolymers* **1971**, *10*, 465−480.
(23) Müller, W.; Crothers, D. M. *J. Mol. Biol.* **1968**, *35*, 251−290.

Table 1. UV–Visible Characteristics of TθOPP in the Presence of [poly(dA-dT)]$_2$

	immediately after mixing					24 h after mixing				
R	λ_{So} (nm)	ϵ_{So} (M^{-1} cm^{-1})	H (%)	A_{So}/A_{sh}	ϵ_{bHP} (M^{-1} cm^{-1})	λ_{So} (nm)	ϵ_{So} (M^{-1} cm^{-1})	H (%)	A_{So}/A_{sh}	ϵ_{bHP} (M^{-1} cm^{-1})
					10 mM PIPES/10 mM NaCl at pH 7.0					
0.25	425	2.5×10^5	17	1.4		426	2.6×10^5	14	1.4	
0.05	424	2.8×10^5	8	1.6	5×10^4	425	3.0×10^5	1	1.6	4×10^4
0.01	424	2.9×10^5	3	1.9	8×10^4	425	3.1×10^5	−5	1.9	8×10^4
					10 mM PIPES/100 mM NaCl at pH 7.0					
0.25	425	2.4×10^5	3	1.3		427	2.4×10^5	5	1.4	
0.05	424	2.8×10^5	−13	1.4		425	2.9×10^5	−15	1.4	
0.01	424	3.0×10^5	−21	1.6	3×10^4	425	3.1×10^5	−23	1.6	3×10^4
					10 mM MES/10 mM NaCl at pH 6.0					
0.25	425	1.8×10^5	58	1.4	1.2×10^5	425	1.8×10^5	58	1.4	1.3×10^5
0.05	426	1.7×10^5	60		1.8×10^5	428	1.1×10^5	75		3.8×10^5
0.01	426	1.7×10^5	61		2.3×10^5	428	1.2×10^5	73		4.1×10^5
					10 mM MES/100 mM NaCl at pH 6.0					
0.25	426	1.9×10^5	21	1.4	6×10^4	426	1.9×10^5	21	1.4	5×10^4
0.05	426	1.6×10^5	37		2.3×10^5	426	1.8×10^5	27		2.0×10^5
0.01	426	1.5×10^5	39		2.5×10^5	426	1.6×10^5	37		2.5×10^5

Table 2. UV–Visible Characteristics of TθOPP in the Presence of [poly(dG-dC)]$_2$

	immediately after mixing					24 h after mixing				
R	λ_{So} (nm)	ϵ_{So} (M^{-1} cm^{-1})	H (%)	A_{So}/A_{sh}	ϵ_{bHP} (M^{-1} cm^{-1})	λ_{So} (nm)	ϵ_{So} (M^{-1} cm^{-1})	H (%)	A_{So}/A_{sh}	ϵ_{bHP} (M^{-1} cm^{-1})
					10 mM PIPES/10 mM NaCl at pH 7.0					
0.25	422	2.1×10^5	31	1.1		422	2.0×10^5	37	1.1	
0.05	422	2.2×10^5	28	1.2		425	2.1×10^5	31	1.2	
0.01	425	2.2×10^5	28	1.2	4×10^4	425	2.4×10^5	24	1.3	3×10^4
					10 mM PIPES/100 mM NaCl at pH 7.0					
0.25	420	1.6×10^5	29	1.1		421	1.5×10^5	35	1.0	
0.05	420	1.6×10^5	29	1.1		421	1.5×10^5	35	1.1	
0.01	429	1.7×10^5	25	1.1		430	1.7×10^5	25	1.1	
					10 mM MES/10 mM NaCl at pH 6.0					
0.25	422	1.8×10^5	60	1.2	5×10^4	423	1.7×10^5	61	1.2	4×10^4
0.05	422	1.2×10^5	73		1.4×10^5	426	9×10^4	80		2.2×10^5
0.01	426	1.0×10^5	79		1.9×10^5	428	9×10^4	80		2.5×10^5
					10 mM MES/100 mM NaCl at pH 6.0					
0.25	420	1.8×10^5	29	1.1		421	1.6×10^5	37	1.1	
0.05	420	1.6×10^5	37	1.1	3×10^4	422	1.5×10^5	41	1.1	3×10^4
0.01	429	1.5×10^5	41	1.2	7×10^4	429	1.5×10^5	41	1.3	6×10^4

at 520, 558, 583, and 640 nm. In addition, the Soret band of **P** exhibits a shoulder at ~396 nm which shifts to ~410 nm upon DNA binding or addition of salt or PIPES buffer. Previously, the ratio of the intensities of the Soret band and its shoulder (A_{So}/A_{sh}) was shown to be an indicator for self-stacking of TθOPP; a lower ratio indicates greater stacking.[16,17] Both the intensity of the Soret band and the A_{So}/A_{sh} ratio are sensitive to conditions which affect self-stacking, *e.g.* salt concentration and presence of PIPES buffer.[17] Protonation of TθOPP (**HP**) leads to a red-shift of the Soret band to 445 nm ($\epsilon = 5.1 \times 10^5$ M^{-1} cm^{-1}) and only two Q bands at 620 and 680 nm. The ϵ values reported are always in units of M^{-1} cm^{-1}, but the units are omitted for brevity.

Studies with [poly(dA-dT)]$_2$. pH 7.0. In order to quantitate the effects of DNA binding on the visible absorbance spectrum of TθOPP, several parameters are presented in Tables 1 and 2: the λ_{max} of the Soret band (λ_{So}), the molar absorptivity of the Soret band (ϵ_{So}), the hypochromicity of the Soret band (H) [H is defined as $[(A_o - A_s)/A_o] \times 100\%$, where A_o and A_s are the absorbances at the Soret λ_{max} without and with added electrolytes, respectively], the ratio of the intensities of the Soret band and its shoulder at ~410 nm (A_{So}/A_{sh}), and the molar absorptivity (ϵ_{bHP}) of the band corresponding to the DNA-bound, protonated TθOPP (**bHP**). The addition of [poly(dA-dT)]$_2$ to a TθOPP solution (7.5 μM TθOPP, pH 7.0, 10 mM PIPES buffer, 10 mM NaCl) caused the Soret band to be red-shifted by 7 nm at $R = 0.25$ and by 6 nm at 0.05 and 0.01 (Figure 1). The ϵ_{So} values decreased by 17%, 8%, and 3% at $R = 0.25$, 0.05, and 0.01, respectively. The A_{So}/A_{sh} values increased with decreasing R. After 1 day, ϵ_{So} values increased for all three R values, and A_{So}/A_{sh} values remained unchanged. In the initial spectra, a small shoulder at 451 nm, characteristic of **bHP**, was observed at $R = 0.05$ and 0.01, with $\epsilon_{451} = 5 \times 10^4$ and 8×10^4, respectively. After 1 day, ϵ_{bHP} decreased slightly to 4×10^4 at $R = 0.05$ and remained unchanged at $R = 0.01$.

In 100 mM NaCl (pH 7.0) (supporting information Figure S1 and Table 1), the ϵ_{So} values were similar to those in 10 mM NaCl. The A_{So}/A_{sh} values were 1.3, 1.4, and 1.6, slightly less than those in 10 mM NaCl. For $R = 0.01$, a small **bHP** band was present with $\epsilon_{bHP} = 3 \times 10^4$. After 1 day, the ϵ_{So} increased slightly at $R = 0.05$ and 0.01; ϵ_{So} remained unchanged at $R = 0.25$. The A_{So}/A_{sh} value increased to 1.4 at $R = 0.25$.

pH 6.0. At pH 6.0 (10 mM MES, 10 mM NaCl) (Figure 2), ϵ_{bHP} values were significantly larger than those at pH 7.0. The A_{So}/A_{sh} value was 1.4 at $R = 0.25$, but the ratio was not measurable at $R = 0.05$ or 0.01 due to the absence of a shoulder. One day later, ϵ_{So} remained unchanged at $R = 0.25$ and decreased at $R = 0.05$ and 0.01. The ϵ_{bHP} values increased after 1 day for all three R values.

The degree of protonation was reduced in 100 mM NaCl (Figure S2). The ϵ_{bHP} values were 6×10^4, 2.3×10^5, and 2.5×10^5 at $R = 0.25$, 0.05, and 0.01, respectively. At $R = 0.25$, the A_{So}/A_{sh} ratio was 1.4. After 1 day, the ϵ_{So} value remained unchanged at $R = 0.25$ and increased slightly at $R = 0.05$ and

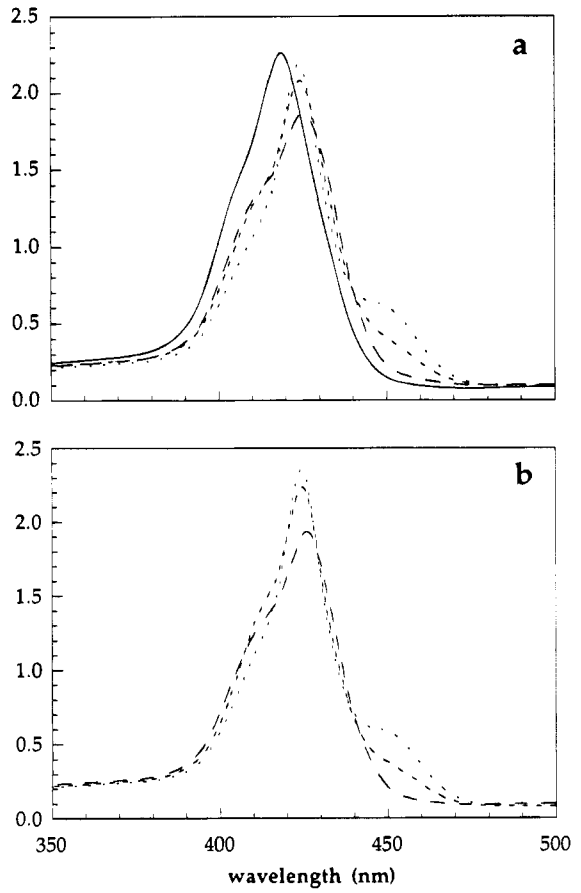

Figure 1. Visible absorbance spectrum of 7.5 μM TθOPP in the presence of [poly(dA-dT)]$_2$: (a) immediately after mixing; (b) 24 h after mixing. Solutions contained 10 mM PIPES (pH 7.0), 10 mM NaCl. Key: no DNA (—); R = 0.25 (— —); R = 0.05 (- - -); R = 0.01 (• • •).

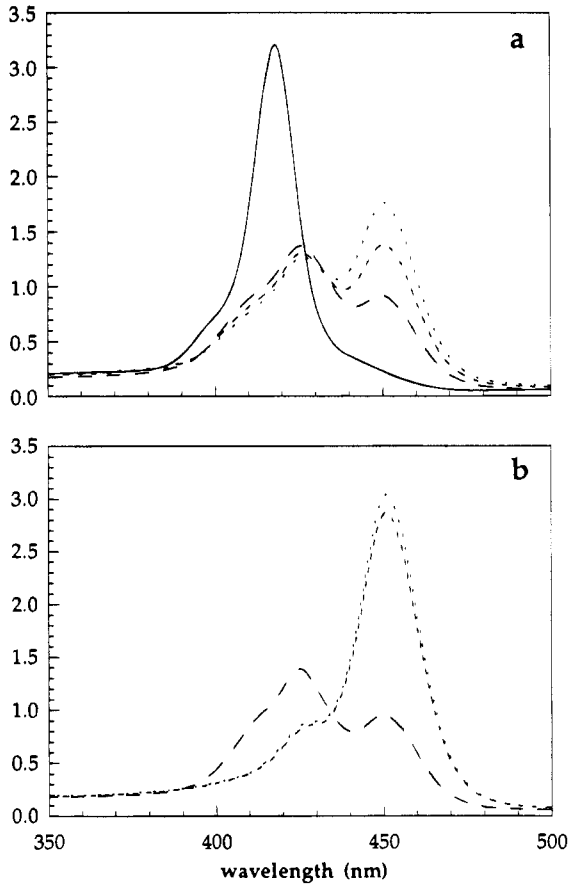

Figure 2. Visible absorbance spectrum of 7.5 μM TθOPP in the presence of [poly(dA-dT)]$_2$: (a) immediately after mixing; (b) 24 h after mixing. Solutions contained 10 mM MES (pH 6.0), 10 mM NaCl. Key: no DNA (—); R = 0.25 (— —); R = 0.05 (- - -); R = 0.01 (• • •).

0.01. The ϵ_{bHP} values decreased at R = 0.25 and 0.05 to 5 × 10^4 and 2.0 × 10^5, respectively; ϵ_{bHP} remained unchanged after 1 day at R = 0.01.

Studies with [poly(dG-dC)]$_2$. pH 7.0. At pH 7.0 (10 mM PIPES, 10 mM NaCl) (Figure 3), at R = 0.25, ϵ_{So} was 2.1 × 10^5 and A_{So}/A_{sh} was 1.1; 1 day later, ϵ_{So} decreased slightly (A_{So}/A_{sh} was unchanged). At R = 0.05, ϵ_{So} was 2.2 × 10^5 (A_{So}/A_{sh} = 1.2); in 1 day, ϵ_{So} decreased slightly and A_{So}/A_{sh} remained unchanged. At R = 0.01, ϵ_{So} = 2.2 × 10^5 immediately after mixing; A_{So}/A_{sh} was 1.2. A small **bHP** band was observed at 454 nm. In 1 day, ϵ_{So} increased to 2.4 × 10^5 and A_{So}/A_{sh} increased to 1.3. Also after 1 day, the intensity of the 454 nm band decreased.

In 100 mM NaCl, the Soret band was very broad with three apparent overlapping peaks at 408, 420, and 430 nm (Figure 4); this spectral shape had not been observed with [poly(dA-dT)]$_2$. Very similar spectra were recorded for R = 0.25, 0.05, and 0.01 (Figure 4). At R = 0.25 and 0.05, ϵ_{420} and ϵ_{430} were both equal to 1.6 × 10^5. At R = 0.01, however, the two bands became less resolved as a band at ~429 nm increased in intensity. The A_{So}/A_{sh} values were 1.1 for all three R values. After 1 day, ϵ_{421} and ϵ_{430} decreased slightly at R = 0.25 and 0.05 but remained unchanged at R = 0.01. There was no band observed at 454 nm.

pH 6.0. At pH 6.0 (10 mM MES, 10 mM NaCl) (Figure S3), the λ_{max} values of the Soret band at R = 0.25 and 0.05 were both 422 nm and, after 1 day, shifted to 423 and 426 nm, respectively. For R = 0.01, the λ_{max} value was shifted from 426 to 428 nm after 1 day. The protonated form appeared as a shoulder at 454 nm; ϵ_{bHP} was 5 × 10^4, 1.4 × 10^5, and 1.9 × 10^5 for R = 0.25, 0.05, and 0.01, respectively. One day later, ϵ_{bHP} decreased at R = 0.25, and ϵ_{bHP} increased for both R = 0.05 and 0.01.

When [NaCl] was increased to 100 mM, the Soret bands were once again quite broad and flat. At R = 0.25, three overlapping peaks were evident centered at 409, 420, and 431 nm (Figure S4). In the R = 0.25 solution, the ϵ_{420} value was initially 1.8 × 10^5 but decreased slightly 1 day later. At R = 0.05, ϵ_{420} was 1.6 × 10^5, and there was also a small **bHP** band at 460 nm. After 1 day, ϵ_{420} decreased to 1.5 × 10^5 and A_{So}/A_{sh} and ϵ_{bHP} remained unchanged. At R = 0.01, the 420 and 431 nm bands formed a single band at 429 nm. The A_{So}/A_{sh} value was 1.2, and ϵ_{bHP} was 7 × 10^4. After 1 day, ϵ_{429} remained unchanged, A_{So}/A_{sh} increased to 1.3, and ϵ_{bHP} decreased.

Circular Dichroism. Studies with [poly(dA-dT)]$_2$. pH 7.0. At pH 7.0 (10 mM PIPES, 10 mM NaCl) (Figure 5 and Table 3), the circular dichroism (CD) spectrum of the TθOPP−[poly(dA-dT)]$_2$ system had the same exciton-type pattern as had been observed for the TθOPP−CT DNA system—a negative band at 423−425 nm (exc1 band)) and a positive band at 435−439 nm (exc2 band), accompanied by a smaller positive band between 400 and 410 nm (s1 band).[17] At R = 0.25, the molar ellipticities were rather large, with $[\Theta]_{exc1}$ = −2.4 × 10^6 and $[\Theta]_{exc2}$ = 1.6 × 10^6. At R = 0.05, $[\Theta]_{exc1}$ and $[\Theta]_{exc2}$ values were very similar to those at R = 0.25. At R = 0.01, $[\Theta]_{exc1}$ and $[\Theta]_{exc2}$ were reduced by approximately 50% from the values at R = 0.25 and 0.05. After 1 day, the $[\Theta]_{exc1}$ values increased for R = 0.25, 0.05, and 0.01. Even though a small **bHP** band had been present in the visible absorbance spectrum, no **bHP** band was apparent in the CD spectrum.

Table 3. Circular Dichroism Characteristics of TθOPP in the Presence of $[poly(dA\text{-}dT)]_2$

	immediately after mixing								24 h after mixing							
R	λ_{s1} (nm)	$[\Theta]_{s1}$ ($\times 10^{-5}$)	λ_{exc1} (nm)	$[\Theta]_{exc1}$ ($\times 10^{-5}$)	λ_{exc2} (nm)	$[\Theta]_{exc2}$ ($\times 10^{-5}$)	λ_{bHP} (nm)	$[\Theta]_{bHP}$ ($\times 10^{-5}$)	λ_{s1} (nm)	$[\Theta]_{s1}$ ($\times 10^{-5}$)	λ_{exc1} (nm)	$[\Theta]_{exc1}$ ($\times 10^{-5}$)	λ_{exc2} (nm)	$[\Theta]_{exc2}$ ($\times 10^{-5}$)	λ_{bHP} (nm)	$[\Theta]_{bHP}$ ($\times 10^{-5}$)
						10 mM PIPES/10 mM NaCl at pH 7.0										
0.25	404	3.2	424	−24.1	436	15.7			403	3.8	425	−28.2	437	17.2		
0.05	407	4.2	424	−24.0	436	15.3			408	5.7	424	−28.7	436	18.4		
0.01	408	2.4	424	−12.7	436	8.5			408	4.7	424	−22.4	436	14.5		
						10 mM PIPES/100 mM NaCl at pH 7.0										
0.25	404	3.3	424	−22.7	436	14.5			404	3.5	425	−24.0	438	13.9		
0.05	408	6.1	424	−33.2	436	21.5			407	6.6	424	−34.6	436	22.4		
0.01	408	4.5	424	−24.7	436	16.0			408	6.2	424	−32.0	436	20.6		
						10 mM MES/10 mM NaCl at pH 6.0										
0.25	405	1.2	425	−8.3	436	5.9	460	1.7	408	2.2	425	−11.3	436	7.5	459	1.6
0.05	405	0.7	424	−4.7	436	3.6	459	2.0			424	−0.2	438	0.6	460	2.5
0.01	405	0.5	425	−2.5	437	2.2	459	2.0							459	2.1
						10 mM MES/100 mM NaCl at pH 6.0										
0.25	405	1.8	425	−13.0	437	7.6			407	2.3	425	−15.3	439	8.8		
0.05	408	1.2	425	−6.3	436	4.6	458	1.6	408	2.1	425	−9.9	436	6.8	458	1.7
0.01	409	0.3	424	−1.4	436	1.7	458	1.6	409	1.1	424	−5.1	436	3.9	457	1.7

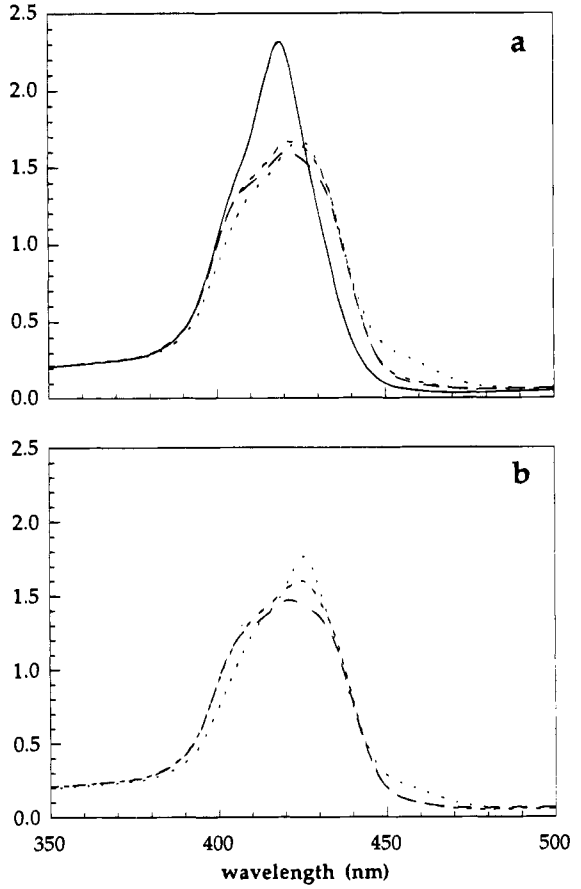

Figure 3. Visible absorbance spectrum of 7.5 μM TθOPP in the presence of $[poly(dG\text{-}dC)]_2$: (a) immediately after mixing; (b) 24 h after mixing. Solutions contained 10 mM PIPES (pH 7.0), 10 mM NaCl. Key: no DNA (—); $R = 0.25$ (– –); $R = 0.05$ (- - -); $R = 0.01$ (•••).

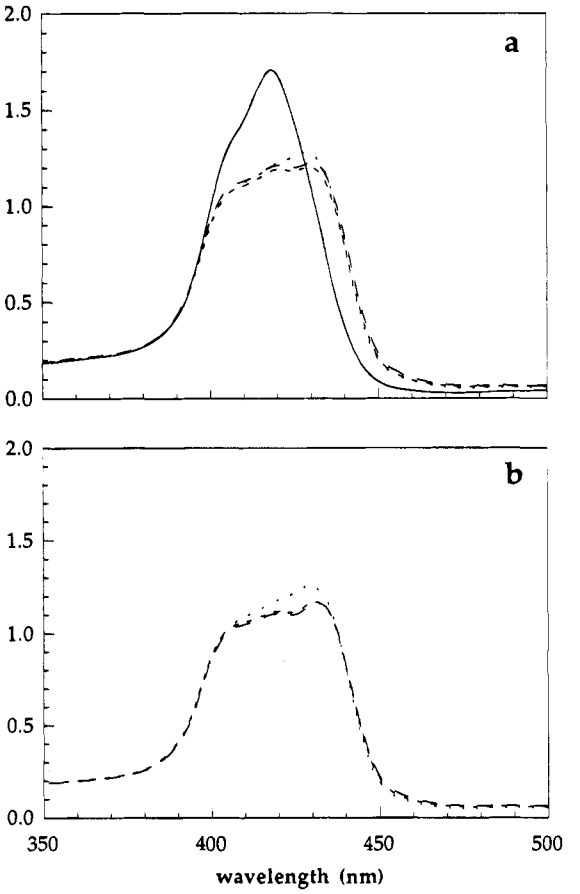

Figure 4. Visible absorbance spectrum of 7.5 μM TθOPP in the presence of $[poly(dG\text{-}dC)]_2$: (a) immediately after mixing; (b) 24 h after mixing. Solutions contained 10 mM PIPES (pH 7.0), 100 mM NaCl. Key: no DNA (—); $R = 0.25$ (– –); $R = 0.05$ (- - -); $R = 0.01$ (•••).

At 100 mM NaCl (pH 7.0, 10 mM PIPES) the molar ellipticities were also quite large (Figure S5). At $R = 0.25$, $[\Theta]_{s1}$, $[\Theta]_{exc1}$, and $[\Theta]_{exc2}$ were 3.3×10^5, -2.3×10^6, and 1.5×10^6, respectively. Changes in the spectrum over 1 day included slight increases in the s1 and exc1 bands and a slight decrease in the exc2 band. At $R = 0.05$, the $[\Theta]_{s1}$, $[\Theta]_{exc1}$, and $[\Theta]_{exc2}$ values were 85%, 43%, and 47% greater than those at $R = 0.25$. After 1 day, they increased slightly. At $R = 0.01$, the molar ellipticities decreased to values similar to those at $R = 0.25$. After 1 day, the band intensities at $R = 0.01$ were larger than those at $R = 0.25$ but smaller than those at $R = 0.05$.

In the UV region of the CD spectrum, $[poly(dA\text{-}dT)]_2$ (pH 7.0, 10 mM PIPES, 100 mM NaCl) has a characteristic conservative spectrum with a negative band at 246 nm and a positive band and shoulder at 260 and 275 nm, respectively (Figure S9). With the addition of 7.5 μM TθOPP ($R = 0.05$),

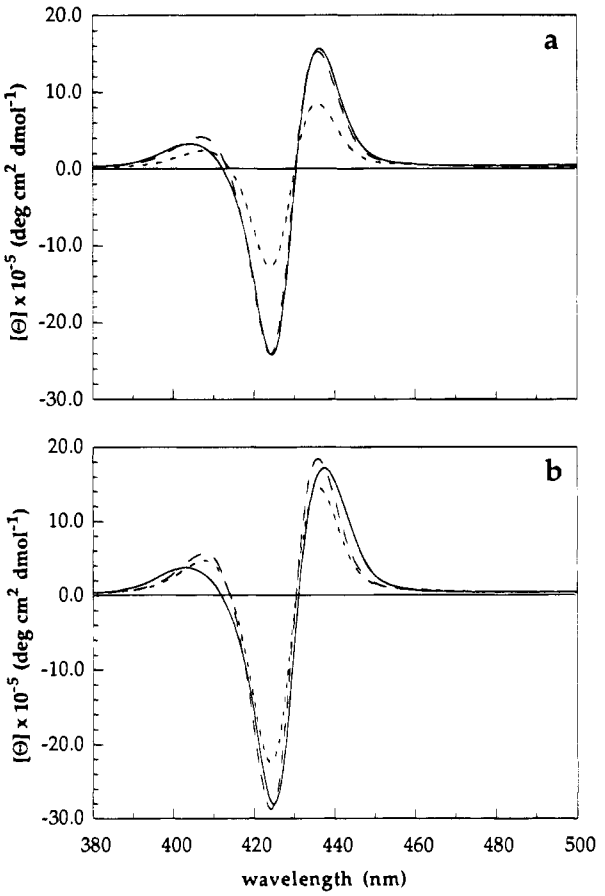

Figure 5. Circular dichroism spectrum of 7.5 μM TθOPP in the presence of [poly(dA-dT)]$_2$: (a) immediately after mixing; (b) 24 h after mixing. Solutions contained 10 mM PIPES (pH 7.0), 10 mM NaCl. Key: $R = 0.25$ (—); $R = 0.05$ (— —); $R = 0.01$ (- - -).

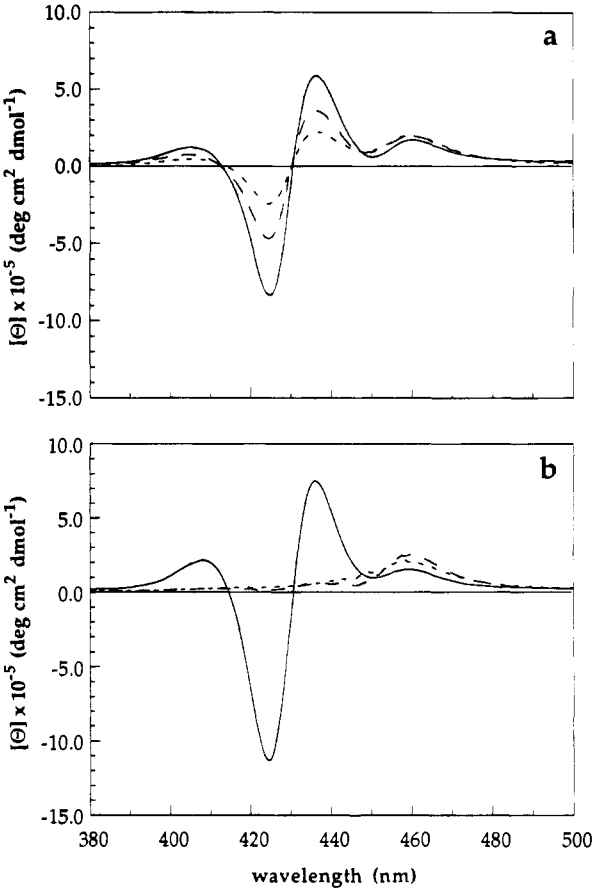

Figure 6. Circular dichroism spectrum of 7.5 μM TθOPP in the presence of [poly(dA-dT)]$_2$: (a) immediately after mixing; (b) 24 h after mixing. Solutions contained 10 mM MES (pH 6.0), 10 mM NaCl. Key: $R = 0.25$ (—); $R = 0.05$ (— —); $R = 0.01$ (- - -).

neither the shape of the spectrum nor the band intensities changed significantly.

pH 6.0. At pH 6.0, 10 mM MES, and 10 mM NaCl (Figure 6), the spectrum consisted of both the exciton signal and a 460 nm band. At $R = 0.25$, the $[\Theta]_{s1}$, $[\Theta]_{exc1}$, and $[\Theta]_{exc2}$ values were 1.2×10^5, -8.3×10^5, and 5.9×10^5, respectively; the **bHP** band at 460 nm had an intensity of 1.7×10^5. The only changes with time were an increase in all three components of the exciton signal and a slight decrease in the **bHP** band. The intensities of the s1, exc1, and exc2 bands decreased with decreasing R. At $R = 0.05$, the spectra were a combination of the 460 nm band and a small conservative signal. The $[\Theta]_{bHP}$ value increased by 25% after 1 day. At $R = 0.01$, the $[\Theta]_{s1}$, $[\Theta]_{exc1}$, and $[\Theta]_{exc2}$ values were the smallest of the three R values, and $[\Theta]_{bHP}$ was 2.0×10^5. After 1 day, the exciton signal was reduced to baseline, and $[\Theta]_{bHP}$ increased to 2.1×10^5.

At pH 6.0 in 100 mM NaCl (Figure S6) protonation was observed at low R. At $R = 0.25$, a strong conservative signal was observed, and after 1 day, the s1, exc1, and exc2 bands increased by 28%, 18%, and 16%, respectively. The initial $R = 0.05$ spectrum had smaller intensities than those at $R = 0.25$. The **bHP** band was at 458 nm with an intensity of 1.6×10^5. After 1 day, the conservative region of the spectrum increased, and $[\Theta]_{bHP}$ increased slightly to 1.7×10^5. At $R = 0.01$, the exciton spectrum was initially low in intensity, but the s1, exc1, and exc2 bands increased by 500%, 260%, and 130%, respectively, after 1 day. The intensity of the **bHP** band was identical to that for $R = 0.05$ both initially and after 1 day.

Studies with [poly(dG-dC)]$_2$. pH 7.0. The addition of [poly(dG-dC)]$_2$ (Figure 7 and Table 4) gave an exciton feature at pH 7.0, 10 mM PIPES, and 10 mM NaCl. At $R = 0.25$, the spectrum taken immediately after sample preparation exhibited the three typical bands at 401, 424, and 436 nm. In addition, next to the negative 424 nm band, there was a negative shoulder (s2 band) at ~416 nm (see pH 6.0 section below). After 1 day, the intensities of the s1 and exc1 bands at $R = 0.25$ remained unchanged, and the exc2 band decreased by 20%. With decreasing R, the exciton signal intensities increased. As the intensities increased, the s2 shoulder disappeared. At $R = 0.01$, the intensities increased dramatically with time to 4.8×10^5, -24.9×10^5, and 16.5×10^5, respectively, after 1 day. Due to the slow time-dependent changes in the spectra, the spectra were re-acquired each day over an 8 day period (data not shown). The $R = 0.01$ exhibited the maximal signal after six days with $[\Theta]_{s1}$, $[\Theta]_{exc1}$, and $[\Theta]_{exc2}$ equal to 8.7×10^5, -4.1×10^6, and 2.5×10^6, respectively.

In 100 mM NaCl (pH 7.0, 10 mM PIPES) (Figure 8), an unusual "inverted" CD signal was observed. The inverted spectrum was comprised of a small negative band at ~400 nm, a larger positive band at 415−420 nm, and a negative band at 430−440 nm ("−s1/+exc1/−exc2"). At $R = 0.25$, the initial signal changed very little over 1 day, except for an increase in intensity of the 419 nm band. This positive band was rather broad with a shoulder at ~405 nm, suggesting the possibility of overlapping bands. At $R = 0.05$, the signal was similar to the initial spectrum at $R = 0.25$ but with slightly larger ellipticities at 398 and 418 nm. After 1 day, the 418 and 434 nm bands increased by 63% and 40%, respectively. At $R = 0.01$, the initial "inverted" spectrum had intensities of $[\Theta]_{s1} = -7 \times 10^4$, $[\Theta]_{exc1} = 2.4 \times 10^5$, and $[\Theta]_{exc2} = -1.5 \times 10^5$. After 1 day, the longer wavelength negative band shifted to

Table 4. Circular Dichroism Characteristics of TθOPP in the Presence of $[poly(dG\text{-}dC)]_2$

	immediately after mixing								24 h after mixing							
R	λ_{s1} (nm)	$[\Theta]_{s1}$ ($\times 10^{-5}$)	λ_{exc1} (nm)	$[\Theta]_{exc1}$ ($\times 10^{-5}$)	λ_{exc2} (nm)	$[\Theta]_{exc2}$ ($\times 10^{-5}$)	λ_{bHP} (nm)	$[\Theta]_{bHP}$ ($\times 10^{-5}$)	λ_{s1} (nm)	$[\Theta]_{s1}$ ($\times 10^{-5}$)	λ_{exc1} (nm)	$[\Theta]_{exc1}$ ($\times 10^{-5}$)	λ_{exc2} (nm)	$[\Theta]_{exc2}$ ($\times 10^{-5}$)	λ_{bHP} (nm)	$[\Theta]_{bHP}$ ($\times 10^{-5}$)
						10 mM PIPES/10 mM NaCl at pH 7.0										
0.25	401	0.5	424	−1.1	436	2.5			401	0.5	425	−1.2	437	2.0		
0.05	402	0.6	425	−1.9	437	3.0			401	1.8	425	−12.2	437	8.8		
0.01	405	0.7	425	−4.2	437	4.1			408	4.8	425	−24.9	437	16.5		
						10 mM PIPES/100 mM NaCl at pH 7.0										
0.25	398	−0.3	419	1.2	433	−1.0			397	−0.2	418	1.7	433	−1.0		
0.05	398	−0.4	418	1.6	434	−1.0			398	−0.3	418	2.6	432	−1.4		
0.01	398	−0.7	417	2.4	437	−1.5			399	−0.7	416	3.5	439	−0.8		
						10 mM MES/10 mM NaCl at pH 6.0										
0.25	401	0.2	424	−1.1	436	1.9	451	0.3	402	0.5	425	−3.1	437	2.8	452	0.3
0.05	404	0.1	425	−0.1	439	1.1	448/465	1.2/−0.6	409	0.6	426	−2.2	438	2.5	448/464	1.5/−0.6
0.01	411	0.1	427	−0.3	439	1.1	448/465	1.2/−0.6	411	0.3	427	−1.0	440	1.5	448/465	1.5/−0.7
						10 mM MES/100 mM NaCl at pH 6.0										
0.25	400	−0.3	418	1.3	435	−0.9			398	−0.2	418	1.4	434	−1.1		
0.05	399	−0.5	417	1.9	437	−1.3			402	−0.4	417	1.4	427/436	−0.2/−0.4		
0.01	398	−0.3	413/426	1.2/−1.2	435	0.4	448/464	0.3/−0.2	410	1.0	425	−4.0	438	2.7		

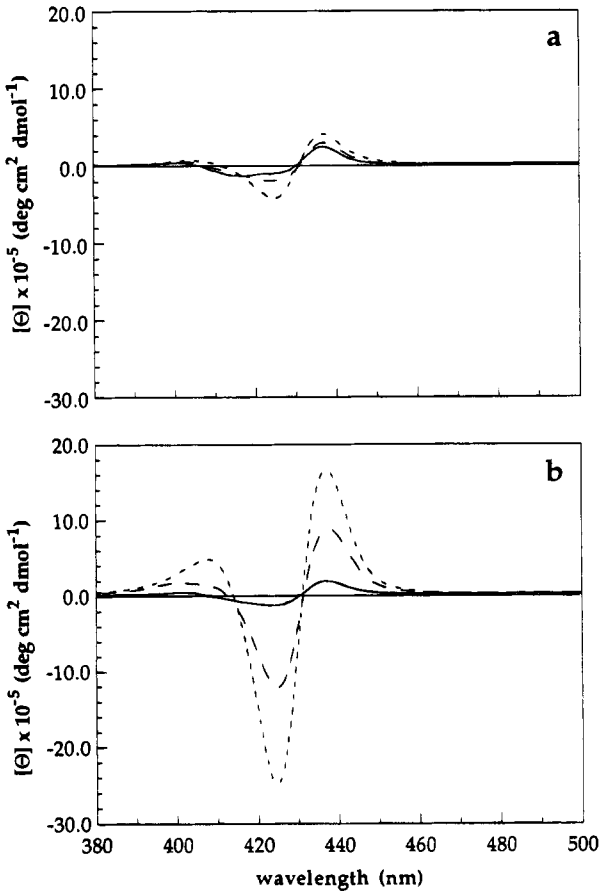

Figure 7. Circular dichroism spectrum of 7.5 μM TθOPP in the presence of $[poly(dG\text{-}dC)]_2$: (a) immediately after mixing; (b) 24 h after mixing. Solutions contained 10 mM PIPES (pH 7.0), 10 mM NaCl. Key: $R = 0.25$ (—); $R = 0.05$ (– –); $R = 0.01$ (- - -).

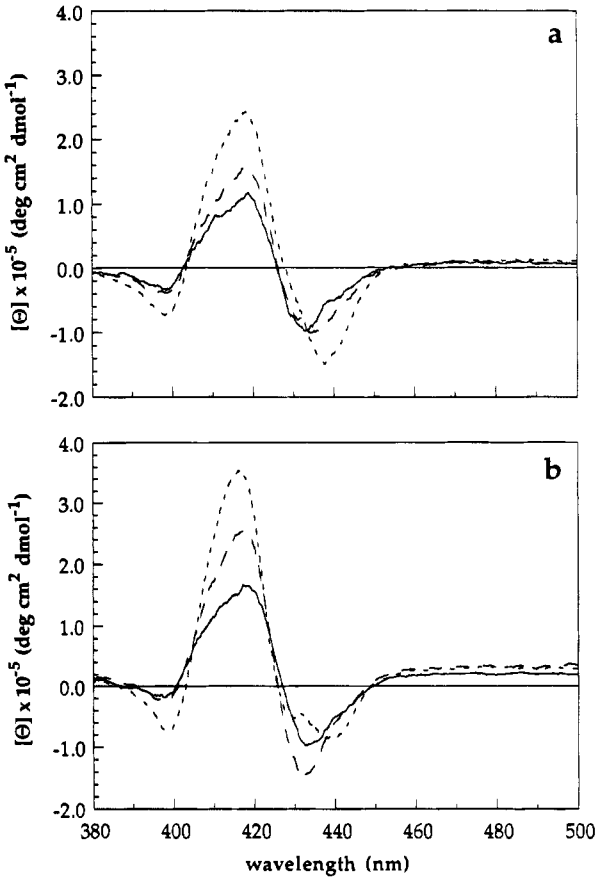

Figure 8. Circular dichroism spectrum of 7.5 μM TθOPP in the presence of $[poly(dG\text{-}dC)]_2$: (a) immediately after mixing; (b) 24 h after mixing. Solutions contained 10 mM PIPES (pH 7.0), 100 mM NaCl. Key: $R = 0.25$ (—); $R = 0.05$ (– –); $R = 0.01$ (- - -).

439 nm and decreased to $[\Theta]_{439} = -8 \times 10^4$. Also, this band appeared to develop a shoulder at ~430 nm. Over several days, the negative band increased in intensity and shifted to 426 nm, and a smaller positive band appeared at 436 nm. These changes may be a partial conversion to the noninverted spectrum.

pH 6.0. At pH 6.0 (10 mM MES, 10 mM NaCl) (Figure 9), several overlapping conservative signals were observed. At $R = 0.25$, a low-intensity conservative signal was observed, with the s2 shoulder at ~410 nm. With time, the intensities of the s1, exc1, and exc2 signals increased, while the negative shoulder at 410 nm disappeared. At $R = 0.05$, the initial conservative signal was small. In the 450–460 nm region of the spectrum, a conservative signal emerged, with a positive band at 448 nm and a negative band at 465 nm. After 1 day, the s1, exc1, and exc2 bands increased in intensity, while the **bHP** bands remained relatively unchanged. At $R = 0.01$, the s1 and exc1 bands were once again small, while the **+bHP** and **-bHP** bands were identical to those at $R = 0.05$. After 1 day, the $[\Theta]_{s1}$, $[\Theta]_{exc1}$, and $[\Theta]_{exc2}$ values increased, while the $[\Theta]_{+bHP}$ and $[\Theta]_{-bHP}$ values were 1.5×10^5 and -7×10^4, respectively.

At both pH 6.0 (Figure 9) and pH 7.0 (Figure 7) the CD

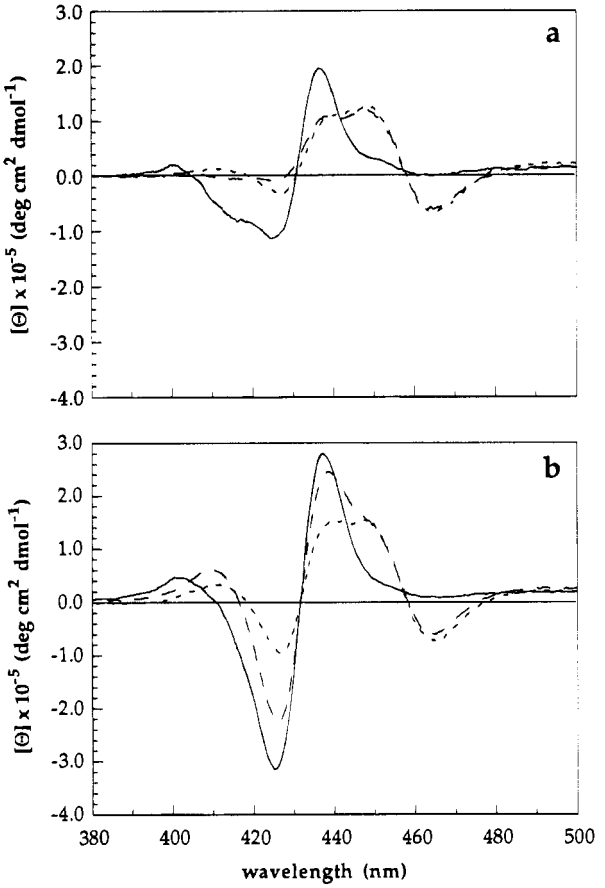

Figure 9. Circular dichroism spectrum of 7.5 μM TθOPP in the presence of [poly(dG-dC)]$_2$: (a) immediately after mixing; (b) 24 h after mixing. Solutions contained 10 mM MES (pH 6.0), 10 mM NaCl. Key: R = 0.25 (—); R = 0.05 (– –); R = 0.01 (- - -).

spectra at R = 0.25 (10 mM NaCl) contained the negative s2 shoulder at ~410 nm; such a shoulder had been seen only transiently and only with CT DNA.[17] It appeared that this negative shoulder was associated with a stacked species of TθOPP, since the shoulder at ~410 nm in the absorbance spectrum is most prominent under conditions favoring self-stacking. The s2 shoulder is at the correct wavelength to possibly be the negative component of an exciton signal, with the positive component at ~400 nm, which would be consistent with an additional stacked species. Unfortunately, the relatively large exc1 band overlaps with the s2 shoulder and as the exc1 band increases in intensity completely obscures the shoulder.

In 100 mM NaCl (Figure S7), an R-dependent conversion from the "inverted" spectral shape to the "+s1/−exc1/+exc2" shape was observed. At R = 0.25, the initial spectrum exhibited the usual "inverted" shape. After 1 day, the only change in the spectrum was slightly more intense signals. At R = 0.05, the inverted CD spectrum had a negative shoulder (399 nm) and a positive (417 nm) and negative (437 nm) conservative band. However, after 1 day, the exc1 band split into two bands at 427 and 436 nm. Also, a small positive shoulder appeared at 448 nm. At R = 0.01, the general shape of the spectrum was inverted, but the exc1 band was shifted to 413 nm, the exc2 band was shifted to 426 nm, and a small positive band appeared at 435 nm. In addition, a small conservative signal was present in the **bHP** region of the spectrum. After 1 day, the spectrum converted to a relatively strong signal with the "+s1/−exc1/+exc2" shape.

Competitive Binding Studies. To investigate preferential binding to [poly(dA-dT)]$_2$ or to [poly(dG-dC)]$_2$, competitive

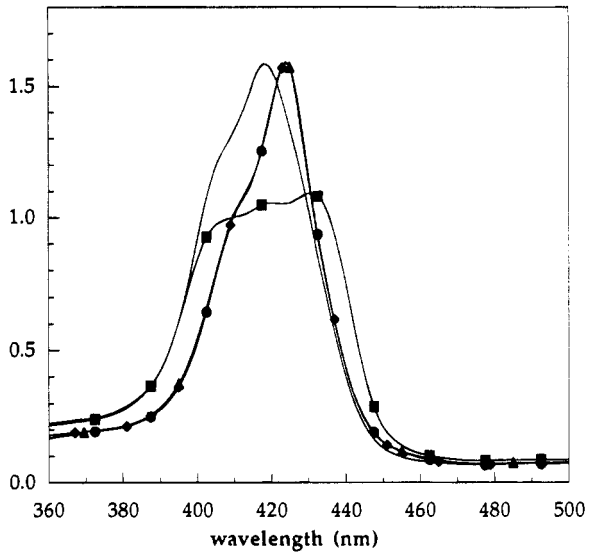

Figure 10. Visible absorbance spectra of 7.5 μM TθOPP in competitive binding study with [poly(dA-dT)]$_2$ and [poly(dG-dC)]$_2$. Samples contained the following: no DNA (—); [poly(dA-dT)]$_2$ only (150 μM in base pairs) (●); [poly(dG-dC)]$_2$ only (150 μM in base pairs) (■); TθOPP−[poly(dA-dT)]$_2$ adduct + [poly(dG-dC)]$_2$ (◆); TθOPP−[poly-(dG-dC)]$_2$ adduct + [poly(dA-dT)]$_2$ (▲).

Chart 2

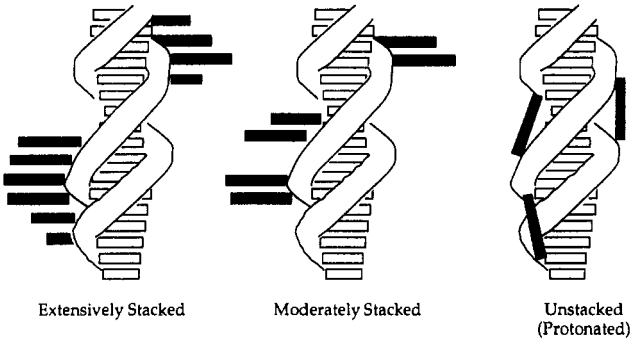

binding studies were performed. First, a solution was prepared with 7.5 μM TθOPP and [poly(dA-dT)]$_2$ at R = 0.05 (pH 7.0, 10 mM PIPES, 100 mM NaCl). The absorbance and CD spectra were acquired (Figure 10 and synopsis illustration), and the sample was allowed to equilibrate for 1 h. Then, an equivalent aliquot of [poly(dG-dC)]$_2$ was added to the solution and caused no significant changes in the absorbance or the CD spectrum of the TθOPP−[poly(dA-dT)]$_2$ adduct. In a similar experiment, [poly(dA-dT)]$_2$ was added to an equilibrated TθOPP−[poly-(dG-dC)]$_2$ solution. Upon addition of [poly(dA-dT)]$_2$, the Soret band immediately changed from the broad, three-maxima shape to the more typical single Soret band with the 410 nm shoulder (Figure 10). In the CD spectrum, the low intensity, inverted spectrum converted immediately to a stronger signal with the +s1/−exc1/+exc2 shape, nearly identical to the spectrum with only [poly(dA-dT)]$_2$ (synopsis illustration).

Discussion

Our previous investigations of TθOPP found that this porphyrin did not intercalate into CT DNA under any of the conditions studied.[15-17] When bound to DNA, the free base form of TθOPP produced a self-stacked DNA adduct (Chart 2). Although the length or size of these aggregates was probably heterogeneous, we observed spectral changes under different conditions which led us to recognize two categories of stacked, DNA-bound TθOPP species:[17] (i) an extensively self-stacked

form, favored at high R values, at higher salt concentrations, and with PIPES buffer; (ii) a moderately self-stacked form, favored at intermediate R values (0.05) and at low salt concentrations. Extensive self-stacking was characterized in the CD spectra by relatively low-intensity conservative signals and in the absorbance spectra by low A_{So}/A_{sh} ratios and hypochromicity of the Soret band. Compared to extensive stacking, moderate stacking was evidenced by a more intense conservative CD band and by slightly larger A_{So}/A_{sh} ratios and less hypochromicity of the Soret band. The exact structural differences between extensive and moderate stacking remain unclear, but since moderate stacking is favored at lower R values, we suspect that the size of the aggregates of the TθOPP species along the DNA surface is smaller for the moderately stacked form. The extent of overlap of the porphyrins may also be different between the two forms. It must be stressed that we believe these are closely similar forms and that neither is homogeneous but must represent a range of cluster sizes. Furthermore, the spectra often appear as mixtures of the two forms, and we believe they coexist but with each form favored under certain conditions noted above. When TθOPP was protonated, the porphyrin appeared to adopt an unstacked outside binding mode with CT DNA. Protonation was favored at low pH, at low salt concentrations, and at low R values.

[poly(dA-dT)]$_2$. The spectral characteristics of TθOPP bound to [poly(dA-dT)]$_2$ reported above were generally similar to those of TθOPP bound to CT DNA [Soret band shifted by 6−7 nm and slight hypochromicity (Figure 1), characteristic +s1/−exc1/+exc2 three-band CD pattern (Figure 5), with the exciton signal indicating outside binding with self-stacking]. Thus, it is likely that the binding of TθOPP to [poly(dA-dT)]$_2$ is similar to that to CT DNA.

For [poly(dA-dT)]$_2$ at pH 7.0, the intensities of the CD bands were larger regardless of R value than for either CT DNA or for [poly(dG-dC)]$_2$ (Figures 5 and S5). The $[\Theta]_{exc1}$ values were consistently greater than -2.0×10^6 at pH 7.0 for [poly(dA-dT)]$_2$. Larger CD signals and higher A_{So}/A_{sh} ratios (Figure 1) are associated with the moderately stacked form of TθOPP.[17] Therefore, the moderately stacked form is favored with [poly(dA-dT)]$_2$.

At pH 7.0, protonation of TθOPP was significant in 10 mM NaCl with [poly(dA-dT)]$_2$; the degree of protonation increased with decreasing R (Figure 1). We found with CT DNA that stacking acted to inhibit protonation of bound TθOPP and that, consequently, factors that increased stacking could decrease the degree of protonation.[17] In 100 mM NaCl, protonation was reduced at all three R values (Figure S1). The similar absorbance spectra and strong conservative CD signals at 10 and 100 mM NaCl indicated that binding was still essentially complete even in 100 mM NaCl, so that the reduced protonation in 100 mM NaCl was probably caused by more favored stacking of bound TθOPP and not by decreased binding.

At pH 6.0, protonation was extensive, as indicated by the intense **bHP** bands (451 nm) in the absorbance spectra (Figures 2 and S2). Generally, protonation increased with time and with decreasing R. However, even though at pH 6.0 the absorbance spectra showed a higher degree of protonation at $R = 0.01$ than at $R = 0.05$, the $[\Theta]_{bHP}$ value in the CD spectrum at $R = 0.01$ was less than (in 10 mM NaCl) or equal to (in 100 mM NaCl) that at $R = 0.05$ (Figures 6 and S6). Since it is unlikely that there is less binding of protonated porphyrin to DNA at $R = 0.01$ than at $R = 0.05$, the lower intensity may result from a different orientation of the bound protonated porphyrin at the different R values.

The comparison of the absorbance and CD spectra acquired immediately after sample preparation to those acquired 1 day later was intended to observe time-dependent changes in the binding of TθOPP to DNA. The differences in the spectra over 1 day for [poly(dA-dT)]$_2$ were relatively small, with the exception of the growth of the **bHP** band in the absorbance spectra at pH 6.0, 10 mM MES, and 10 mM NaCl (Figure 2). All samples were also re-analyzed 2 h after sample preparation (data not shown), and nearly all time-dependent changes in the spectra of the [poly(dA-dT)]$_2$ samples were complete within 2 h. On the other hand, significant changes were observed in the [poly(dG-dC)]$_2$ samples over the course of many days. Therefore, not only was binding of TθOPP with [poly(dA-dT)]$_2$ preferential over that with [poly(dG-dC)]$_2$ but the equilibrium of binding with [poly(dA-dT)]$_2$ was achieved on a relatively faster time scale.

[poly(dG-dC)]$_2$. In contrast to the spectral results with [poly(dA-dT)]$_2$, which have many similarities to those with CT DNA, we found that TθOPP binding gave broad Soret bands and low-intensity and sometimes inverted CD signals with [poly(dG-dC)]$_2$, indicating a different type of binding of TθOPP to [poly(dG-dC)]$_2$ compared to [poly(dA-dT)]$_2$ and CT DNA.

In 10 mM NaCl at pH 7.0, the Soret bands (Figure 3) were broad with low A_{So}/A_{sh} ratios (1.1−1.3), consistent with the extensive self-stacking binding mode of TθOPP. For the same samples, the low intensities of the exc1 ($[\Theta]_{exc1} = -4.2 \times 10^5$ at $R = 0.01$) and exc2 ($[\Theta]_{exc2} = 4.1 \times 10^5$ at $R = 0.01$) CD bands (Figure 7) immediately after sample preparation also suggested this binding mode. After 1 day, the ϵ_{So} values increased for both $R = 0.05$ and 0.01, and the Soret band became narrower at $R = 0.01$. The conservative CD signals also increased dramatically after 1 day at $R = 0.05$ and 0.01. These results indicate that with [poly(dG-dC)]$_2$, extensive self-stacking of TθOPP was favored, particularly at $R = 0.25$. At lower R values, partial conversion to the moderately stacked form occurred but on a relatively slow time scale.

Binding of TθOPP in 100 mM NaCl (pH 7.0, 10 mM PIPES) produced uniquely different absorbance and CD spectra. In this higher salt concentration, the Soret region (Figure 4) was very broad and had at least three overlapping bands at 408, 420, and 430 nm. The Soret bands at $R = 0.25$, 0.05, and 0.01 were relatively similar in shape and intensity, findings which indicate essentially complete binding. However, the unusual inverted shape of the CD spectrum (Figure 8) suggests that the bound TθOPP is oriented differently than the self-stacked, DNA adduct that is formed with [poly(dA-dT)]$_2$ or with CT DNA; this inverted CD spectrum was observed only with [poly(dG-dC)]$_2$ at 100 mM NaCl. However, several observations suggest that, at lower R (0.01), at least a small fraction of the bound TθOPP was in a form which was similar to the more commonly observed stacked forms. With time, the amount of this more normal form increased. These observations include the following: (1) a slight prominence of a single maximum at 429 nm; (2) a larger intensity of the 429 nm band than that at $R = 0.25$ and 0.05, which increased with time; (3) over several days, a gradual conversion of the CD spectrum to a more typical strong conservative signal with a negative band at 426 nm and a positive band at 436 nm. The 418 nm positive band of the inverted CD spectrum decreased in intensity and shifted to 412 nm, even though it never disappeared completely. However, as the CD spectrum changed, the Soret bands did not change very much, suggesting that the minor form has a much stronger CD intensity than the major form responsible for the majority of the Soret band.

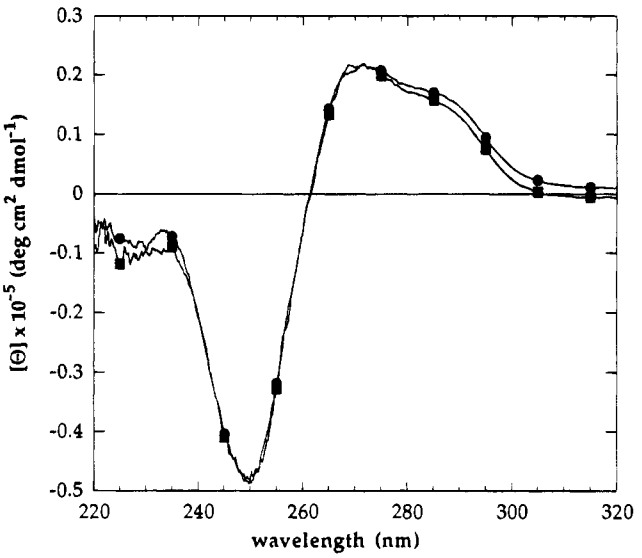

Figure 11. Comparison of the UV-region circular dichroism spectra of [poly(dG-dC)]$_2$ only (150 μM in base pairs) (●) and the TθOPP–[poly(dG-dC)]$_2$ adduct (R = 0.05) (■) in which the visible-region circular dichroism spectrum is inverted (pH 7.0, 10 mM PIPES, 100 mM NaCl).

An inversion of the induced CD signal may suggest a change in the conformation of the DNA itself. [poly(dG-dC)]$_2$ is known to undergo a conversion from right-handed DNA to left-handed Z-DNA with the addition of high salt concentrations.[24] Moreover, *meso*-tetrakis(4-*N*-methylpyridiniumyl)porphyrin (TMpyP-(4)) can convert Z-form [poly(dG-dC)]$_2$ back to the *B*-form upon intercalation.[25] In the UV region of the spectrum (240–300 nm), the left-handed Z-DNA exhibits an inverted CD spectrum compared to that of the right-handed DNA. The UV CD spectrum of the TθOPP–[poly(dG-dC)]$_2$ adduct (R = 0.05) that produced the inverted visible CD spectrum has the same shape as the spectrum of the right-handed [poly(dG-dC)]$_2$ (Figure 11). This same spectral shape was observed up to R = 0.25. The lack of any changes in the CD signals associated with [poly-(dG-dC)]$_2$ itself indicates that the conformation of the DNA was not altered by binding to TθOPP under these conditions.

At pH 6.0 (10 mM MES, 10 mM NaCl) with [poly(dG-dC)]$_2$ (Figures S3 and 9), the Soret bands were once again rather broad, suggesting extensive self-stacking of TθOPP. The ~410 nm negative shoulder in the CD spectrum, associated with extensive self-stacking, was observed at R = 0.25. Protonation was indicated by a 451 nm band, even though protonation was less extensive than with [poly(dA-dT)]$_2$ or with CT DNA. In the CD spectrum, the signal associated with the DNA bound, protonated form of TθOPP (**bHP**) is conservative, indicative of self-stacking of **bHP**. A self-stacked form of **bHP** had not been observed with either [poly(dA-dT)]$_2$ or with CT DNA. Self-stacking of protonated porphyrins has been observed but for the anionic porphyrin *meso*-tetrakis(4-sulfonophenyl)porphyrin (in the absence of DNA).[26] In our studies with CT DNA,[17] it appeared that the added positive charge from protonation of the core of a cationic porphyrin disfavored stacking of **bHP**. However, for [poly(dG-dC)]$_2$, self-stacking of **bHP** may be stabilized enough by the DNA template to overcome the added electrostatic repulsion from the positive charge of the proton.

At pH 6.0 in 100 mM NaCl (Figures S4 and S7), the Soret band was broad with three overlapping maxima, as found at pH 7.0 in 100 mM NaCl (Figure 4), consistent with extensive self-stacking of TθOPP when bound to [poly(dG-dC)]$_2$ in 100 mM NaCl. The CD spectrum was also inverted at R = 0.25 and 0.05 immediately after sample preparation, suggesting that the differently oriented form of DNA-bound TθOPP was formed at this pH also. However, at R = 0.01, a positive band had begun to develop at 435 nm and the negative band was shifted to 426 nm. After 1 day, the CD spectrum at R = 0.01 had completely converted to the more typical +s1/–exc1/+exc2 shape, whereas, at pH 7.0, several days had been necessary for only partial conversion. In addition, after 1 day the R = 0.05 spectrum also showed signs of conversion, i.e., splitting of the negative band at ~430 nm and the development of a small positive band at ~440 nm. When these samples were re-analyzed after 6 days, both the R = 0.05 and 0.01 spectra had completely converted to the +s1/–exc1/+exc2 shape. Therefore, conversion to the usual stacked form of TθOPP is favored at lower pH as well as at lower R.

Comparison of TθOPP Binding to Different DNAs. [poly-(dG-dC)]$_2$ is less flexible than [poly(dA-dT)]$_2$ in solution, as indicated by NMR studies of exchangeable imino protons of DNA[27,28] and by torsional rigidity measurements.[29] Bound TθOPP stacking is more extensive with [poly(dG-dC)]$_2$ than with either [poly(dA-dT)]$_2$ or CT DNA, as evidenced by broad Soret bands and low-intensity CD signals. With high salt concentration (100 mM NaCl), the self-stacked TθOPP was oriented differently on the DNA backbone as evidenced by the inverted, induced visible CD spectrum.

The competitive binding studies clearly indicated that TθOPP binds selectively to [poly(dA-dT)]$_2$. The addition of [poly(dG-dC)]$_2$ to the TθOPP–[poly(dA-dT)]$_2$ adduct caused no change in the absorbance or CD spectra (Figures 10 and S8), suggesting that all of the TθOPP remains associated with [poly(dA-dT)]$_2$. The immediate change in the absorbance and CD spectra of the TθOPP–[poly(dG-dC)]$_2$ complex upon addition of [poly-(dA-dT)]$_2$ also indicated that TθOPP dissociated from [poly-(dG-dC)]$_2$ and preferentially bound to [poly(dA-dT)]$_2$. The absorbance and CD spectra of TθOPP bound to CT DNA[17] are quite similar to those observed with [poly(dA-dT)]$_2$. This similarity may suggest that TθOPP binds selectively to AT-rich regions of CT DNA.

Competitive binding studies of VOTMpyP(4) and ZnTMpyP-(4) with [poly(dG-dC)]$_2$ and [poly(dA-dT)]$_2$ showed preferential binding to [poly(dA-dT)]$_2$ as found here for TθOPP.[9,12] However, these MTMpyP(4) complexes have an axial ligand and do not engage in extensive self-stacking. Furthermore, the positive N^+CH_3 groups are held in a rigid position. Binding of these MTMpyP(4) complexes to [poly(dA-dT)]$_2$ and to CT DNA caused distinct changes in the UV CD signal of the DNA, indicating distortion of the DNA.[12] On the basis of such UV CD comparisons, the more rigid polymer, [poly(dG-dC)]$_2$, appeared to be less readily distorted by binding with VOTMpyP-(4) (ZnTMpyP(4) was not studied). Interestingly, binding of TθOPP in 100 mM NaCl to [poly(dA-dT)]$_2$ (Figure S9) and to [poly(dG-dC)]$_2$ (Figure 11) produced no change in the UV CD spectrum of the DNA, indicating no significant distortion of

(24) Pohl, F. M.; Jovin, T. M. *J. Mol. Biol.* **1972**, *67*, 375–396.
(25) Pasternack, R. F.; Sidney, D.; Hunt, P. A.; Snowden, E. A.; Gibbs, E. J. *Nucleic Acids Res.* **1986**, *14*, 3927–3943.
(26) Ohno, O.; Kaizu, Y.; Kobayashi, H. *J. Chem. Phys.* **1993**, *99*, 4128–4139.
(27) Early, T. A.; Kearns, D. R.; Hillen, W.; Wells, R. D. *Biochemistry* **1981**, *20*, 3756–3764.
(28) Early, T. A.; Kearns, D. R.; Hillen, W.; Wells, R. D. *Biochemistry* **1981**, *20*, 3764–3769.
(29) Millar, D. P.; Robbins, R. J.; Zewail, A. H. *J. Chem. Phys.* **1981**, *74*, 4200–4201.

the DNA structure. Therefore, the reasons for the differences in binding characteristics of TθOPP to these DNAs must lie elsewhere.

We believe that a more likely explanation involves the differences in the shape, electrostatic potential, and hydration of the grooves of these two polymers. TθOPP showed the same preference for outside binding at AT over GC sites that outside binding MTMpyP(4) derivatives have demonstrated.[9,12] Therefore, we first analyze the role of groove binding for MTMpyP(4) derivatives. Both ZnTMpyP(4) and MnTMpyP(4) have been found to bind in the minor groove of AT regions of DNA,[30,31] and the results suggested that the minor groove binding of MnTMpyP(4) was associated with a melted or partially melted region of the DNA.[31] The changes in the UV CD DNA spectra of the derivatives of TMpyP(4) (M = VO, Zn) combined with the evidence for minor groove binding suggests that such MTMpyP(4) derivatives are bound in the minor groove with some DNA distortion to optimize electrostatic interactions. The minor groove of [poly(dG-dC)]$_2$ is wider than that of [poly(dA-dT)]$_2$ and has a less negative electrostatic potential.[3] Also, the 2-amino group of G is in the minor groove. Therefore, normally minor groove binding for [poly(dG-dC)]$_2$ is less favorable. Binding in the minor groove by MTMpyP(4) derivatives could contribute to sequence selectivity. Indeed, it has been concluded recently that MnTMpyP(4) can bind in the major groove of [poly(dG-dC)]$_2$ since calculations suggest this groove has the most negative potential of all the DNA grooves.[32]

Since the TθOPP species self-stacks in its adducts, the interactions with the grooves could involve the charged groups. In addition to the differences in the grooves themselves, sequence has an effect on the hydration of DNA. Even binding differences for the simple metal cation, Mg^{2+}, have been attributed to such differences in hydration state.[33] Thus, it is not difficult to understand why a tentacle porphyrin could still exhibit selectivity in binding to an undistorted DNA polymer. Likewise, even if the porphyrin is not oriented by a groove, the differences on the surfaces of the polymer could lead to differently oriented species. Thus, such differences could explain the unusual inverted visible CD spectrum observed with [poly(dG-dC)]$_2$ in 100 mM NaCl. The generally weaker CD bands and different Soret region for other conditions of binding to [poly(dG-dC)]$_2$ are also consistent with differences in binding compared to [poly(dA-dT)]$_2$. Finally, similar explanations apply to the differences found between the extent of protonation and the spectral characteristics of TθOPP bound to [poly(dG-dC)]$_2$ compared to [poly(dA-dT)]$_2$ and CT DNA.

Conclusions

We have determined the DNA base pair selectivity of a porphyrin with long, flexible tentacles, TθOPP. We suspected that the ability of the tentacles to conform to the DNA template would limit binding selectivity and that the bound form would be independent of sequence. However, TθOPP displayed not only preferential binding to [poly(dA-dT)]$_2$ over [poly(dG-dC)]$_2$, but also a differently self-stacked species when bound to [poly(dG-dC)]$_2$, especially in 100 mM NaCl. The spectral characteristics and extent of protonation of TθOPP were very similar for [poly(dA-dT)]$_2$ and CT DNA, suggesting preferential AT site binding to this heterogeneous DNA.[17] Therefore, base pair selectivity is still evident, even with the charges on the tentacle arms.

The free base form of TθOPP outside binds to [poly(dA-dT)]$_2$ preferentially in a moderately stacked form, and the protonated form of TθOPP outside binds to [poly(dA-dT)]$_2$ in an unstacked fashion. When bound to [poly(dG-dC)]$_2$, the degree of porphyrin self-stacking is generally greater than with [poly(dA-dT)]$_2$, especially at high salt. When bound to [poly(dG-dC)]$_2$, protonated TθOPP may be self-stacked, as indicated by the conservative CD signal in the **bHP** region of the spectrum. A conservative induced CD feature of protonated TθOPP has not been observed previously. Slow changes in the spectra of the TθOPP−[poly(dG-dC)]$_2$ adduct over several days suggest slow kinetics of a process probably involving partial unstacking of TθOPP. The faster changes observed for [poly(dA-dT)]$_2$ could be due to the lower degree of self-stacking. In higher salt concentrations with [poly(dG-dC)]$_2$, several unusual spectral features of TθOPP were observed, including a broad Soret band with three overlapping maxima and an inverted CD exciton signal. These new features are consistent with an extensively self-stacked TθOPP species with an orientation different from the more usual orientation. The different forms observed for [poly(dG-dC)]$_2$ adducts of both TθOPP and protonated TθOPP compared to adducts with AT-containing polymers may exist because of differences in the major and minor grooves and the associated differences in hydration state. The differences in binding mode, sequence selectivity, coordination number, etc., observed previously for MTMpyP(4) may also be affected by these differences in the grooves and the hydration state. However, the often larger associated changes in DNA polymer structure may mask the effects. Tentacle porphyrins may be better probes of initial polymer structure.

Acknowledgment. This work was supported by the National Institutes of Health Grant AI-127196. We thank Dr. Min Sook Kim for the preparation of TθOPP, and N.E.M. thanks Dr. Srinivasan Mukundan, Jr., for helpful discussions. Instrumentation was funded by NIH and NSF.

Supporting Information Available: Figures of vis and CD spectra of TθOPP−[poly(dA-dT)]$_2$ in high salt, vis spectra of TθOPP−[poly(dG-dC)]$_2$ in low and high salt at pH 6.0, and CD spectra of TθOPP−[poly(dG-dC)]$_2$ in high salt at pH 6.0 and from the competitive binding study (9 pages). Ordering information is given on any current masthead page.

(30) Ward, B.; Skorobogaty, A.; Dabrowiak, J. C. *Biochemistry* **1986**, *25*, 7827−7833.
(31) Raner, G.; Ward, B.; Dabrowiak, J. C. *J. Coord. Chem.* **1988**, *19*, 17−23.
(32) Kuroda, R.; Tanaka, H. *J. Chem. Soc., Chem. Commun.* **1994**, 1575−1576.
(33) Buckin, V. A.; Kankiya, B. I.; Rentzeperis, D.; Marky, L. A. *J. Am. Chem. Soc.* **1994**, *116*, 9423−9429.

IC941072S